Shakedown and Ratcheting Analysis of Printed Circuit Heat Exchangers under Multiple Cyclic Mechanical and Thermal Loads

Jun Shen[a,1] , Zhiyuan Ma[b,1], Haofeng Chen[b,c*]

[a]*School of Energy and Power Engineering, University of Shanghai for Science and Technology, Shanghai 200093, China*

[b]*Department of Mechanical and Aerospace Engineering, University of Strathclyde, Glasgow G1 1XJ, UK*

[c]*Key Laboratory of Pressure Systems and Safety (DOE), School of Mechanical and Power Engineering, East China University of Science and Technology, Shanghai, 200237, China*

Abstract

Printed Circuit Heat Exchangers (PCHEs) is a kind of compact plate heat exchanger with a lot of fine channels in a solid block, called PCHE core. It can withstand high temperature and high pressure. And beyond that, it has many advantages, such as high heat exchange efficiency, low pressure drop, high compactness, good corrosion resistance, long service life and many other advantages. However , PCHEs will endure complex mechanical and thermal loads in service. Meanwhile, shakedown and ratcheting assessment, especially how to determine shakedown and ratcheting boundary for PCHEs in an efficient and accurate way, is still an intractable problem so far. This article makes deep research and analysis to shakedown and ratcheting boundary for PCHEs subjected to complex cyclic load combinations as well as the effect of channel shape and size effects based on the linear matching method (LMM). The influences of load parameters, e.g. temperature difference and pressure difference between hot and cold channels, and geometric parameters, e.g. channel radii, channel shapes, arrangement of channels, and transition radius of the local corner of the semicircular channel, were all discussed in detail. Based on these different types of influence parameters, two-dimensional shakedown and ratcheting boundaries for different kinds of PCHEs models under complex mechanical-thermal load combinations are presented in this paper. It is demonstrated that pressure differences between the hot and cold channel have significant effect, but different channel radii are not so significant. Core size and channel shape are observed to influence the shakedown and ratcheting responses significantly, however, the corner radius shows more significant effect on the shakedown boundary than the ratcheting limit boundary. The PCHE core arrangement, i.e. total number and position, is also found to influence the shakedown and ratcheting responses significantly, especially for the constant pressure loading case. Based on a series of LMM analysis results, it can be concluded that accumulative incremental plastic strain will occur at the region between the cold and the hot channel when the combination of mechanical and thermal loads exceeds the ratcheting limit, which should be under strict control. The results from current parametric studies can be an effective reference for design and optimization of the diffusion bonded PCHE channels in high temperature nuclear applications.

Keywords

Shakedown; Ratcheting; Linear Matching Method (LMM); PCHE; Cyclic loading

* Corresponding authors: haofeng.chen@strath.ac.uk

1 Introduction

With the development of nuclear energy system, the problem of high efficiency heat transfer has attracted much attention. PCHE is a new type of high efficiency heat exchanger. With the advantages of high heat exchange efficiency, low pressure drop, high compactness, PCHE is expected to become an attractive option for nuclear power, solar thermal power generation, coal-based power generation, liquefied air energy storage and other industrial fields. Although different in shape from typical tube-shell heat exchangers, PCHE also contains the following typical components: headers, nozzles, and flanges, as shown in Fig. 1 (a). Fig. 1(b) shows a typical cross section of bonded configure with two semicircular etched channels in one plate. There is another plate bonded at the location of the diameter of the semicircle to construct a channel shown in black area. As for PCHEs, the operating conditions and structural characteristics are both complex, and they usually operate under the combination of high temperature and pressure with cyclic variations. Simultaneously, the cold and hot flow exchanged across the adjacent channels could induce the temperature differences combined with pressure differences.

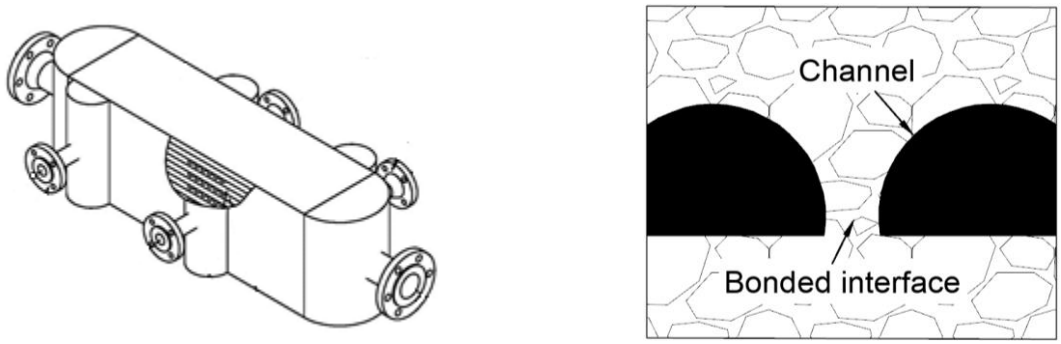

(a) Typical configuration of PCHE **(b) Schematic diagram of a bonded configure** [1]

Fig. 1 The Outline of a PCHE and bonded section

A PCHE core is formed with hot channel plates and cold channel plates which are superimposed together alternately as shown in Fig. 2(a). The semicircular channels on the surface of metal plates are formed by chemical etch.The connection type between plates is diffusion bond and large-scale integration [2]. The bond areas are between the plates. Hot and cold flow channels are distributed in certain ways, such as cross distribution as shown in Fig.2(b). Such configure and manufacturing process can ensure that the PCHE can withstand high temperature, high pressure and the combination of both as well as excellent heat transfer performance.

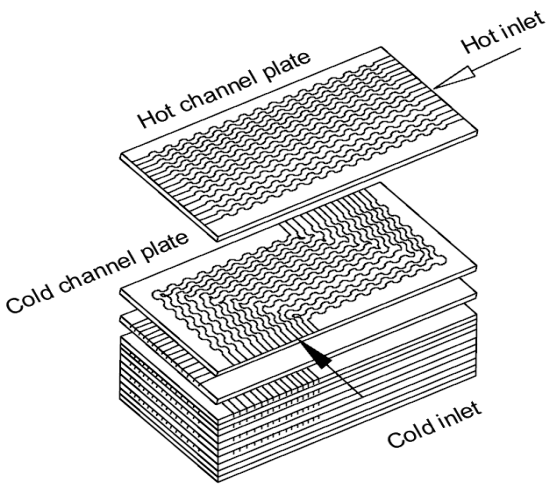

(a) Plate stacking prior to diffusion bonding [2]

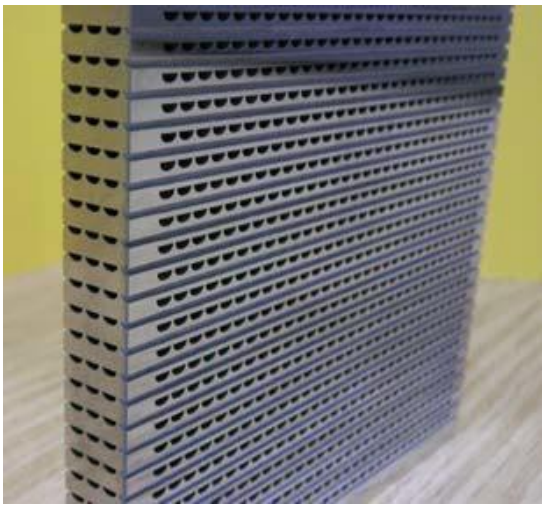

(b)PCHE core with Bonded plate superimposed together [1]

Fig. 2 The Outline of a PCHE core

The problem of thermal stress ratcheting failure is a common and classical problem in chemical, petrochemical, nuclear and other industries. Especially, it is an important failure mechanism for pressurized component. Ratcheting is an accumulated inelastic deformation or strain. Ratcheting may occur when a component subjected to cyclic mechanical stress, thermal stress, or their combination [3]. When cyclic thermal stress existed, thermal stress ratcheting may happen. In detail, thermal stress ratcheting can be caused by a constant mechanical load combined with a strain controlled cyclic load or temperature distribution that is alternately applied and removed. In the process of such cyclic loading, the potential incremental growth of plastic deformation and strain may cause not only ratcheting but also fatigue, which could finally result in plastic collapse or rupture.

Therefore shakedown analysis and ratcheting assessment are important and necessary procedures to ensure the safety of the PCHEs themself and even the whole nuclear plant component. During the normal operation, the PCHEs work under steady temperature and pressure. However, while shut down, start up or other abnormal operating cases happen, they will be subjected to a large temperature gradient and a big change of pressure [4]. Ratcheting, especially thermal stress ratcheting, is one of the most dangerous failure modes. The assessment of shakedown and ratcheting for such a complex structure is a severe problem often encountered in the engineering design, which involves various combinations of thermal and mechanical loads, many structural parameters and construction details. The cold channel angle and the semi-ellipse aspect ratio are two important factors of the performance for PCHEs. The effects of two significant geometric parameters had been analyzed using three-dimensional Reynolds-averaged Navier–Stokes equations [2]. A simplified modeling of thermal ratcheting analyses had been developed based on a system which provided the thermohydraulic behavior inside of PCHEs. The creep and ratcheting coupling of PCHEs were also studied with several scholars, and the results were obtained by parameterization method to simulate the behavior of the creep-fatigue interaction [5-7]. Besides, the experimental heat transfer characteristics of two-phase flow boiling in zigzag channels of PCHE were analyzed to obtain new experimental data and critical conditions of flow pattern transitions, where a new heat transfer correlation for zigzag channels is proposed [8-9]. As refer to the harsh condition encountered in high temperature and high pressure, it is essential to study the effect of different parameters by using finite element method [10]. Many studies have

shown that the calculation of heat transfer performance of PCHEs has been relatively perfect and mature, but there are still defects and limitations in the analysis and evaluation of failure modes under mechanical-thermal loading [11-16]. Since the pressure drop and heat transfer efficiency strongly affect the performance of PCHEs, it is necessary to perform geometric parametric calculation and analysis based on optimization techniques. But for complex structures and load combinations history, it is often huge time-consuming by using incremental finite element method and sometimes hard to judge whether the convergence is achieved. The study in this paper is making efforts to introduce the developed Linear Matching Method (LMM) to predict and evaluate the shakedown and ratcheting boundary accurately and effectively. In order to optimize the performance of PCHEs, it is necessary to investigate effects of different structural parameters, such as diameter of channel, corner radius, core size, channel shape and arrangement of channels based on the LMM analysis.

The LMM, with good numerical stability, high accuracy and efficiency, is very applicable for thermal stress ratcheting assessment of complex practical engineering structures under multi-dimensional loading domain [18][19]. The shakedown–ratcheting boundary diagrams for different kinds of industrial application examples were obtained by several researchers to reveal the characteristics of shakedown and ratcheting response by using the LMM [20-22]. In this study, the LMM procedure was utilized to analyze the shakedown and ratcheting boundary of PCHEs by detailed parametric studies. The influences of key geometric parameters and load combinations were investigated systematically. It can be seen from these studies that the LMM is very suitable for solving shakedown and ratcheting problems of practical engineering equipment or its components under all kinds of loads in industrial applications. Additionally, the obtained results, based on the shakedown and ratcheting boundary of PCHEs subjected to cyclic temperature and mechanical loads, can provide guidance and reference for parametric optimization, structural design and safety operation.

2 The numerical procedure of shakedown and ratcheting analyses using the LMM algorithm

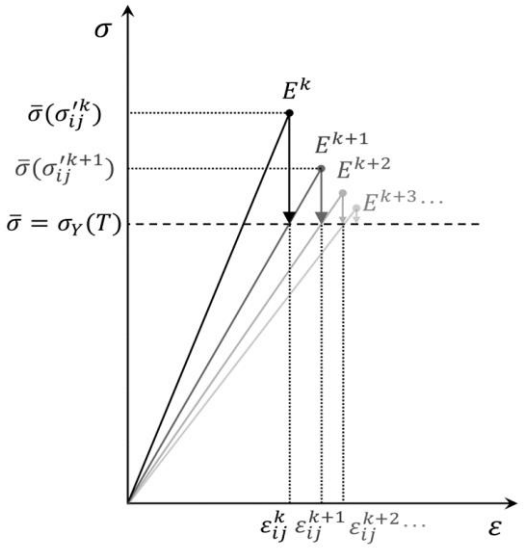

Fig. 3 The matching procedure of the LMM

The LMM, one kind of direct methods, has powerful fuctions in the calculation and evaluation of

several kinds of structural responses considering the effect of material nonlinearity and complex loading. Based on the LMM, the structural plastic behavior is simulated by a series of linear elastic analyses with modified elastic modulus. A schematic matching procedure of the LMM is shown in Fig. 3, where the nonlinear elastic-plastic behavior of material can be substituted by a linear material model in an iterative solution scheme. The principle of the LMM is to use the direct algorithm to the shakedown and ratcheting limits based on both the upper bound and lower bound theorems. At the same time, the equilibrium and compatibility will be satisfied. The validity and robustness of the LMM has been proved by several studies based on ABAQUS step-by-step analysis [20-22]. The following describes the basic principles and numerical procedures of the LMM.

2.1 Cyclic load history

Considering a body with volume V and surface S, subjected to a varying thermal load $\lambda_\theta\theta(x,t)$ in V and a varying mechanical load $\lambda_P P(x,t)$ on part of surface S_P. On the other part of S, denoted by S_U, satisfies the zero-displacement condition. Both thermal and mechanical loads have an identical period T. For a typical time cycle $0 \le t \le t_0$, the problem of a body with external loads can be described as:

$$\hat{\sigma}_{ij}(x,t) = \lambda_p \hat{\sigma}_{ij}^{P}(x,t) + \lambda_\theta \hat{\sigma}_{ij}^{\theta}(x,t) \tag{1}$$

where $\hat{\sigma}_{ij}^{P}(x,t)$ denotes the linear elastic stress solution of $P(x,t)$ while $\hat{\sigma}_{ij}^{\theta}(x,t)$ denotes the linear elastic stress solution of $\theta(x,t)$. Suppose structural material satisfies the Drucker's theorem, the steady-state stress and strain rate under cyclic loads becomes:

$$\sigma_{ij}(t) = \sigma_{ij}(t+\Delta t), \dot{\varepsilon}_{ij}(t) = \dot{\varepsilon}_{ij}(t+\Delta t) \tag{2}$$

For arbitrary cyclic history, the stress solution $\sigma_{ij}(x_k,t)$ is given by:

$$\sigma_{ij}(x,t) = \lambda \hat{\sigma}_{ij}(x,t) + \bar{\rho}_{ij}(x) + \rho_{ij}^{r}(x,t) \tag{3}$$

where λ is the load multiplier; $\bar{\rho}_{ij}(x)$ is a constant residual stress field; $\rho_{ij}^{r}(x,t)$ is a varying residual stress field in each cycle, which satisfies:

$$\rho_{ij}^{r}(x,0) = \rho_{ij}^{r}(x,\Delta t) \tag{4}$$

2.2 The minimum theorem of the LMM

The shakedown and ratcheting analyses are based on the theorem of energy minimization, which is given by:

$$\begin{aligned} I\left(\Delta\varepsilon_{ij}^{n},\lambda\right) &= \sum_{n=1}^{N}\int_{V}\left[\sigma_{ij}^{n}\Delta\varepsilon_{ij}^{n} - \left(\lambda\hat{\sigma}_{ij}(t_n) + \bar{\rho}_{ij} + \rho_{ij}^{r}(t_n)\right)\Delta\varepsilon_{ij}^{n}\right]dV \\ \rho_{ij}^{r}(t_n) &= \sum_{l=1}^{n}\Delta\rho_{ij}^{r}(t_l) \end{aligned} \tag{5}$$

where $\Delta\varepsilon_{ij}^{n}$ denotes the strain increment at load instance $n(n=1\sim N)$; N is the number of load instances in each cycle.

2.2.1 The global minimization process for shakedown analysis

The minimization of $I\left(\Delta\varepsilon_{ij}^{n},\lambda\right)$ is based on a premise that the sum of plastic strain increment in a cycle satisfies strain compatibility. At the k^{th} iteration, suppose a series of plastic strain increment $\Delta\varepsilon_{ij}^{nk}$ is known, a linear elastic material can then be defined with shear modulus $\bar{\mu}^{nk}$ to ensure the stress state reaches yield surface at a given strain state:

$$\frac{3}{2}\bar{\mu}^{nk}\bar{\varepsilon}\left(\Delta\varepsilon_{ij}^{nk}\right)=\sigma_y \tag{6}$$

where $\bar{\varepsilon}$ denotes the von Mises equivalent strain.

For the shakedown analysis, the varying residual stress field in a cycle remains zero: $\rho_{ij}^{r}=0$. Thus the cyclic stress history for the shakedown problem is given by:

$$\sigma_{ij}\left(x,t\right)=\lambda\hat{\sigma}_{ij}\left(x,t\right)+\bar{\rho}_{ij}\left(x\right) \tag{7}$$

A series of incompressible linear relations are then proposed:

$$\Delta\varepsilon_{ij}^{n(k+1)\prime}=\frac{1}{2\bar{\mu}^{nk}}\left[\lambda\hat{\sigma}_{ij}^{\prime}\left(t_n\right)+\bar{\rho}_{ij}^{k+1\prime}\right] \tag{8}$$

where the superscript $'$ indicates deviatoric variables. By summing the linear equations in each cycle, we have:

$$\Delta\varepsilon_{ij}^{(k+1)\prime}=\sum_n\Delta\varepsilon_{ij}^{n(k+1)\prime}=\frac{1}{2\bar{\mu}^{k}}\left[\lambda\sigma_{ij}^{in\prime}+\bar{\rho}_{ij}^{k+1\prime}\right] \tag{9}$$

where $\Delta\varepsilon_{ij}^{(k+1)}=\sum_n\Delta\varepsilon_{ij}^{n(k+1)}$ is the summation of strain increment in a cycle; $\bar{\mu}^{k}$ is calculated by $\frac{1}{\bar{\mu}^{k}}=\sum_n\frac{1}{\bar{\mu}^{nk}}$; σ_{ij}^{in} is calculated by $\sigma_{ij}^{in}=\bar{\mu}^{k}\sum_n\frac{\lambda\hat{\sigma}_{ij}\left(t_n\right)}{\bar{\mu}^{nk}}$. After a number of iterations with (9), the minimization of $I\left(\Delta\varepsilon_{ij}^{n},\lambda\right)$ is reached, where $I\left(\Delta\varepsilon_{ij}^{n(k+1)},\lambda\right)\le I\left(\Delta\varepsilon_{ij}^{n(k)},\lambda\right)$.

2.2.2 The two-step minimization process for ratcheting analysis

The loading condition of the LMM for ratcheting analysis is restricted, so that it can be decomposed into a constant load $\lambda\hat{\sigma}_{ij}^{\bar{F}}\left(x\right)$ and a cyclic load $\hat{\sigma}_{ij}^{\Delta}\left(x,t\right)$. The ratcheting analysis is achieved by a two-step minimization process: the first step is to determine the structural residual stress and plastic strain evolution history for the given cyclic load; the second step is to calculate the limit of the additional constant load, which adopts the same algorithm as the shakedown analysis.

The calculation procedure of residual stress and plastic strain history is given as follows. Suppose the residual stress and plastic strain history of last iteration is known, define a linear elastic equation in deviatoric format as follows:

$$\Delta\varepsilon_{ij}^{Tn(k+1)\prime}=\frac{1}{2\mu}\Delta\rho_{ij}^{n(k+1)\prime}+\Delta\varepsilon_{ij}^{n(k+1)\prime} \tag{10}$$

$$\Delta\varepsilon_{kk}^{Tn(k+1)}=\frac{1}{3K}\Delta\rho_{kk}^{n(k+1)} \tag{11}$$

$$\Delta\varepsilon_{ij}^{n(k+1)\prime}=\frac{1}{2\bar{\mu}^{nk}}\left[\hat{\sigma}_{ij}^{\Delta}\left(t_n\right)+\rho_{ij}\left(t_{n-1}\right)+\Delta\rho_{ij}^{n(k+1)}\right]^{\prime} \tag{12}$$

where,

$$\rho_{ij}\left(t_{n-1}\right)=\rho_{ij}\left(t_0\right)+\sum_{l=1}^{n-1}\Delta\rho_{ij}^{l},\quad \rho_{ij}\left(t_0\right)=\bar{\rho}_{ij}^{0} \tag{13}$$

The iteration procedure is comprised of a number of cyclic analyses, which contains N sub-iterations, where N equals the number of vertices in a loading space. At the first iteration, the residual stress field $\Delta\rho_{ij}^{1}$ is calculated based on the structural response to the first load instance. $\Delta\rho_{ijm}^{n}$ denotes the residual stress field at the m^{th} cycle and n^{th} load instance, where $n=1,2,\cdots,N$ and $m=1,2,\cdots,M$. If the structural response converges at the M^{th} cycle, the structure then reaches steady-

state and the sum of varying residual stress field at N^{th} load instance equals zero. Therefore, the constant residual stress field $\rho_{ij}(t_0)=\bar{\rho}_{ij}^{0}$ after each cycle is given by:

$$\bar{\rho}_{ij}^{0}=\sum_{m=1}^{M}\sum_{n=1}^{N}\Delta\rho_{ijm}^{\ n} \tag{14}$$

The plastic strain amplitude at time point t_n is then given by:

$$\Delta\varepsilon_{ij}^{p}(t_n)=\frac{1}{2\bar{\mu}^{n}}\left[\hat{\sigma}_{ij}^{\Delta\prime}(t_n)+\rho_{ij}'(t_n)\right] \tag{15}$$

where $\bar{\mu}^{n}$ refers to shear modulus at current iteration; $\rho_{ij}(t_n)$ indicates the converged residual stress at time point t_n, where

$$\rho_{ij}(t_n)=\bar{\rho}_{ij}^{0}+\sum_{k=1}^{n}\Delta\rho_{ijM}^{\ k} \tag{16}$$

2.3 The determination of limit multipliers

2.3.1 Shakedown limit multiplier

Based on the upper-bound theorem, the shakedown limit multiplier can be calculated using the following formula.

$$\lambda^{S}=\frac{\int_V\left(\sum_{n=1}^{N}\sigma_{ij}^{n}\Delta\varepsilon_{ij}^{n}\right)dV}{\int_V\left(\sum_{n=1}^{N}\hat{\sigma}_{ij}(t_n)\Delta\varepsilon_{ij}^{n}\right)dV}=\frac{\int_V\left(\sigma_y\sum_{n=1}^{N}\bar{\varepsilon}\left(\Delta\varepsilon_{ij}^{n}\right)\right)dV}{\int_V\left(\sum_{n=1}^{N}\hat{\sigma}_{ij}(t_n)\Delta\varepsilon_{ij}^{n}\right)dV} \tag{17}$$

By (17) , a series of monotonically descending load multipliers can be obtained. These load multipliers eventually approach the actual shakedown limit.

2.3.2 Ratcheting limit multiplier

After determining the steady-state residual stress and plastic strain as given in section 2.2.2, the ratcheting limit multiplier can then be calculated based on the upper-bound equation considering a varying residual stress field:

$$\lambda^{R}=\frac{\int_V\sum_{n=1}^{N}\sigma_y\bar{\varepsilon}\left(\Delta\varepsilon_{ij}^{n}\right)dV-\int_V\sum_{n=1}^{N}\left(\hat{\sigma}_{ij}^{\Delta}(t_n)+\rho_{ij}(t_n)\right)\Delta\varepsilon_{ij}^{n}dV}{\int_V\hat{\sigma}_{ij}^{\bar{F}}\sum_{n=1}^{N}\Delta\varepsilon_{ij}^{n}dV} \tag{18}$$

The differences of both shakedown and ratcheting limit multipliers between each consequent iterations are computed and the relative error after each iteration is compared with a convergence parameter, i.e. 0.001. If the relative error is small enough to satisfy the convergence criterion, the whole process is terminated and the final load multiplier is exported as the converged result.

3 Finite element analysis model of PCHE

PCHE has a very small volume but high heat transfer efficiency, so it is very suitable for the next generation of nuclear power plants and has great potential. The detail design criteria of PCHEs operating under monotonic loading is well established in ASME Code, Section VIII [23]. However, thermal stress ratcheting assessment, especially how to obtain shakedown and ratcheting boundary of PCHEs subjected to multiple cyclic mechanical and thermal loads, is still an intractable problem. So

far there are few references about it. Currently there is no assessment methodologies or design guidance for PCHEs in Section III [24] for nuclear applications. In this paper, several types of small PCHE core plates are designed to investigate the shakedown and ratcheting behaviors for PCHEs in industrial applications by using the LMM. Several geometric parameters represented of actual size PCHE core and loading parameters came from possible service conditions are selected to perform a wide range of parametric calculations.

The application of Koiter's shakedown theorem produces an upper bound shakedown and ratcheting limit to ensure that the actual shakedown limit is always smaller or equal to the upper bound load multipliers. However, during the iteration process, the upper bound load multipliers are proved to continuously decrease to approach the exact shakedown limit multipliers [25]. When converged, the resulting load multiplier could be considered as an infinite range approximation of the exact shakedown or ratcheting limit multiplier.

3.1 Geometry

Two-dimensional, isothermal plain strain analyses are built on the PCHE cross-section, assuming a symmetric boundary condition, to simulate the PCHE ratcheting failure. And there is a small radius on semicircular channel sharp corner to improve numerical convergence.

Considering the symmetry of structure characteristic and loading type, only a half of the PCHE cross-section is established. Fig. 4 shows the symmetric boundary conditions are used on finite element model. For example, the bencnmark model is designed with eight rows and eight columns of semicircular channels with actual representative size PCHE core, as shown in Fig.4a. The mesh discretization consists of 48153 elements and 149606 nodes. The mesh around channel edge (Fig.4b) is denser to ensure the accuracy of analysis results and better convergence in this local region. The temperature distribution was calculated using the 20-node quadratic brick elements (ABAQUS DC3D20) and the structural analysis was performed based on the 20-node quadratic brick elements with reduced integration (ABAQUS C3D20R), respectively.

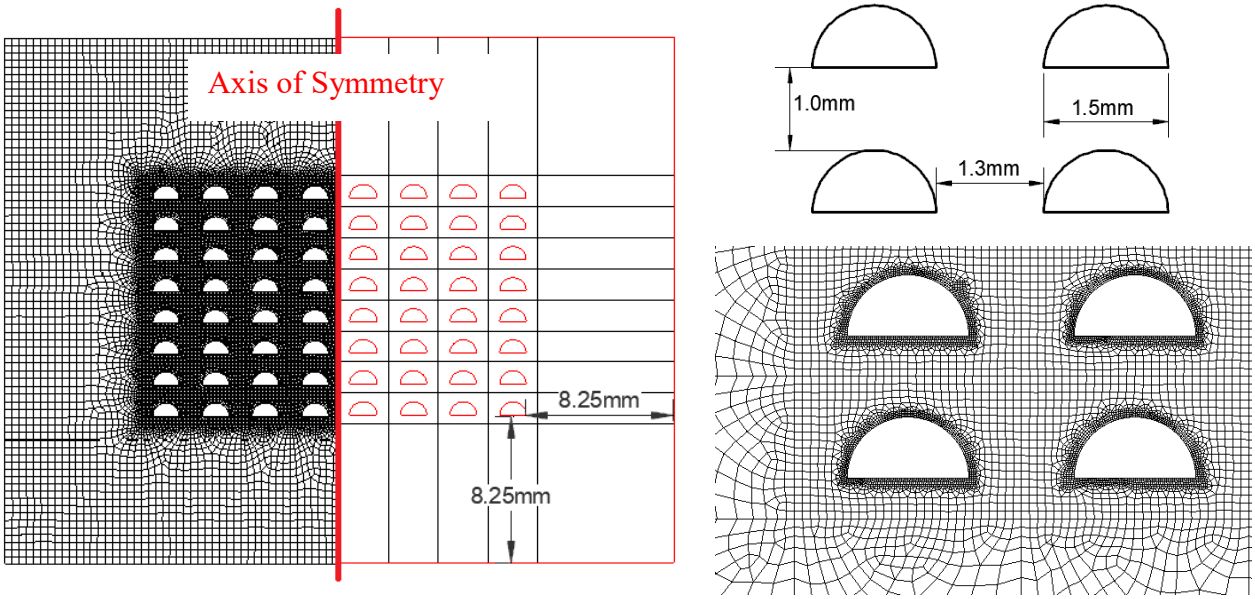

(a) An actual representative PCHE core **(b) The size and mesh of PCHE core**

Fig. 4 Benchmark model of a PCHE core used in this study

3.2 Material

The material property data, i.e. Elastic modulus, Poisson's ratio and so on, is listed in Tab.1. The structural analysis is performed based on an elastic-perfectly plastic material model with small displacement theory and the von-Mises yield function and associated flow rule. With the development of the LMM framework, the consideration of limited kinematic hardening materials has been implemented in the LMM shakedown subroutine [26]. Ramberg-Osgood (R-O) model has also been implemented in the LMM ratcheting subroutine to describe the cyclic hardening effect [27]. In addition, the consideration of temperature-dependent properties is natively supported by the LMM subroutine for shakedown and ratchet analysis [28]. But for the sake of simplicity and conservativeness, only the elastic-perfectly plastic material model with temperature-independent material parameters are adopted for this case.

Tab.1 Material property

Item	Value
Density [kg/m^3]	8100
Elastic modulus [MPa]	2.1E5
Poisson's ratio	0.3
Coefficient of thermal expansion [mm/mm·℃]	1.8E-5
Thermal conductivity [W/(m·℃)]	18
Yield stress [MPa]	200

3.3 Pressure and temperature

The start-up, shut-down and abnormal operating case during whole operating period are considered in this study. For the purpose of conveniently simulating these impormtant processes, it is assumed that the temperature history $\theta(t) = \theta_0 + \Delta\theta(t)$ in the odd rows of PCHE channels follows the curve in Fig. 5 and the temperature history $\theta_0(t) = \theta_0$ in the even rows of PCHE channels remains constant, where room temperature $\theta_0 = 22°C$; A constant internal pressure $P_0 + \Delta P$ has been applied in the odd rows of PCHE channels as shown in Fig.5， and the constant internal pressure in the even rows of PCHE channels is P_0, which is 1 MPa. For example, for a 8X8 benchmark model, the first, third, fifth, and seventh rows are subjected to high temperature and high pressure; the second, fourth, sixth and eighth rows are subjected to low temperature and low pressure. The reference temperature difference $\Delta\theta_0 = 300°C$ and the reference pressure $\Delta P_0 = 6$ MPa. It is worth mentioning that, in the upcoming figures, the pressure difference $\Delta P(=\lambda_p \Delta P_0)$ is normalized by $\Delta P/\sigma_Y$, and the temperature difference $\Delta\theta(=\lambda_\theta \Delta\theta_0)$ is normalized by $Ec\Delta\theta/\sigma_Y$, where σ_Y denotes yield stress, E denotes Young's modulus, and c denotes the thermal expansion coefficient.

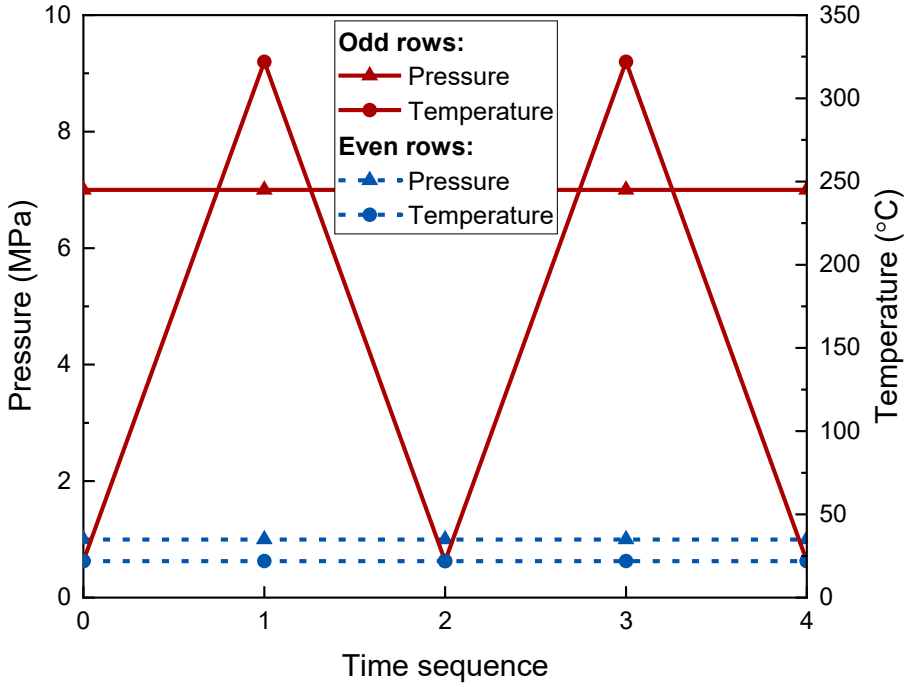

Fig. 5 The reference load history considered for the shakedown and ratcheting analyses of PCHE channels

4 Results and verification

Shakedown and ratcheting analyses of 8×8 PCHE core with corner radius of 5% channel diameter subjected to different pressures and temperatures are performed by using the LMM, as shown in Fig. 6. The diagram has been splited into three regions: for load points within the shakedown limit, the structural behavior is elastic or shakedown; for load points above the shakedown limit but within the ratcheting limit, the structural behavior is alternating plasticity result in the low cycle fatigue damage; for load points outside the ratcheting limit, the structural behavior is ratcheting leading to an incremental plastic collapse. Three different load points in different regions have been chosen for the verification purpose via ABAQUS step-by-step analysis.

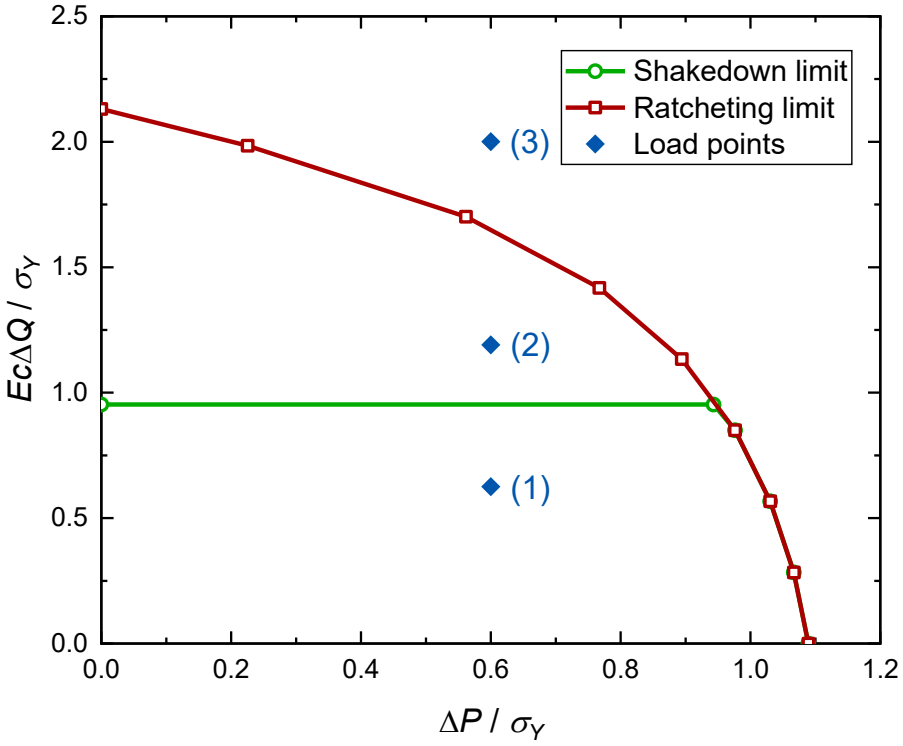

Fig.6 Shakedown and ratcheting boundaries for the 8×8 PCHE core

A total of 50 steps have been created in ABAQUS/CAE to simulate the plastic strain history of the 8×8 PCHE core subjected to the cyclic thermal load and constant pressure load. After job completion, the largest plastic strain magnitude (PEMAG) in the structure is plotted for three different load points, as shown in Fig. 7, which verifies the shakedown and ratcheting boundaries (Fig. 6) calculated by the proposed LMM and calculation model. It can be seen that for load point (1) in the shakedown region, the plastic strain remains constant after a few cycles, demonstrating an expected shakedown behavior. For load point (2) in the alternating plasticity region, the plastic strain remains cyclic but converges to a certain level as expected for the alternating plasticity mechanism. For load point (3) in the ratcheting region, the plastic strain keeps growing for increasing step time, clearly demonstrating a ratchting mechanism as expected.

In addition, a limit analysis has been performed by using the ABAQUS RIKS analysis to verify the limit load of the 8X8 PCHE core subjected to the pressure load. The limit load obtained by the ABAQUS RIKS analysis is identical with that of LMM, where both limit pressure differences ΔP equal to 218MPa. To further validate the efficiency and applicability of the proposed LMM, the CPU time required for a typical LMM analysis is compared with that required for an alternative step-by-step analysis. For load points on the ratchet boundary, the average CPU time required for a complete step-by-step analysis is 11370 seconds while the average CPU time required for a LMM ratchet analysis is 1823.2 seconds. Although the time period of step-by-step analysis depends on the number of steps configured in the FE model, the LMM has proved to be much more efficient than the ABAQUS step-by-step analysis. Therefore, by performing the step-by-step verification, the accuracy of the shakedown and ratcheting boundaries calculated by the LMM has been successfully proven.

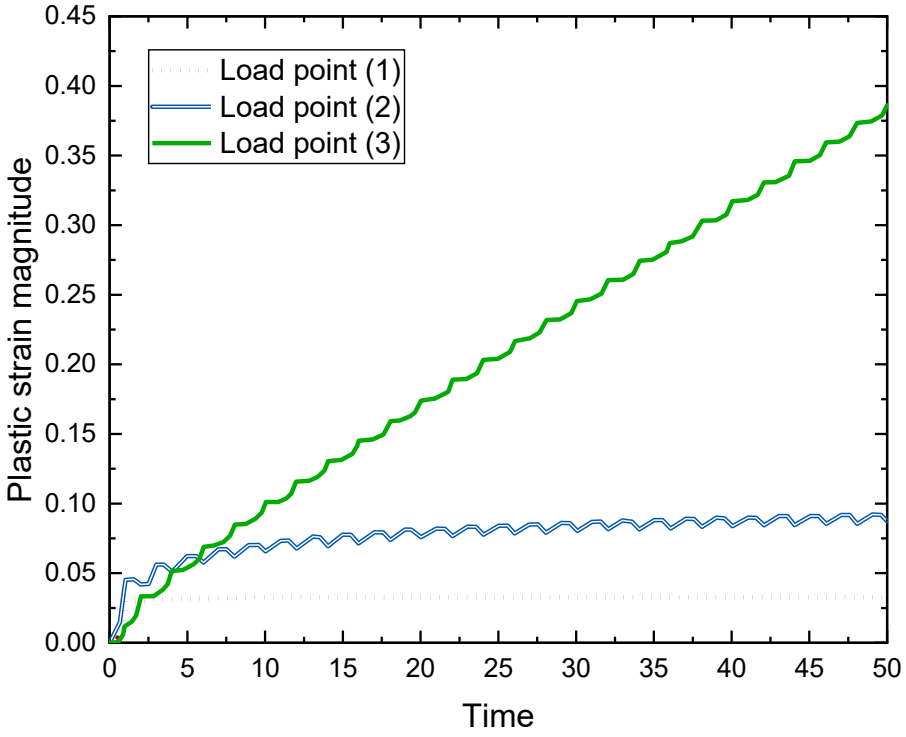

Fig.7 The evolution of plastic strain magnitude for three load points

5 Parametric studies and discussions

5.1 Diameter of channel

Different diameters of 1.3mm,1.5mm,1.8mm and 2mm are modelled to investigate the effect of diameter of channel. The shakedown and ratcheting boundaries for various diameters of channel are summarized in Fig.8. Diameter of channel is observed to have a significant influence on ratcheting boundary, whereas a little influence on shakedown boundary. With the increase of channel diameter, the ratcheting boundary shifts to reduce the shakedown region, and the bearing capacity of PCHE core is weaker. It is worth noting that the ratcheting limit boundary corresponds to the global ratcheting, instead the horizontal shakedown limit (i.e. reverse plasticity limit) boundary is associated with the local alternating plasticity. The size or diameter of channel affects much more on the global ratcheting than the local alternating plasticity.

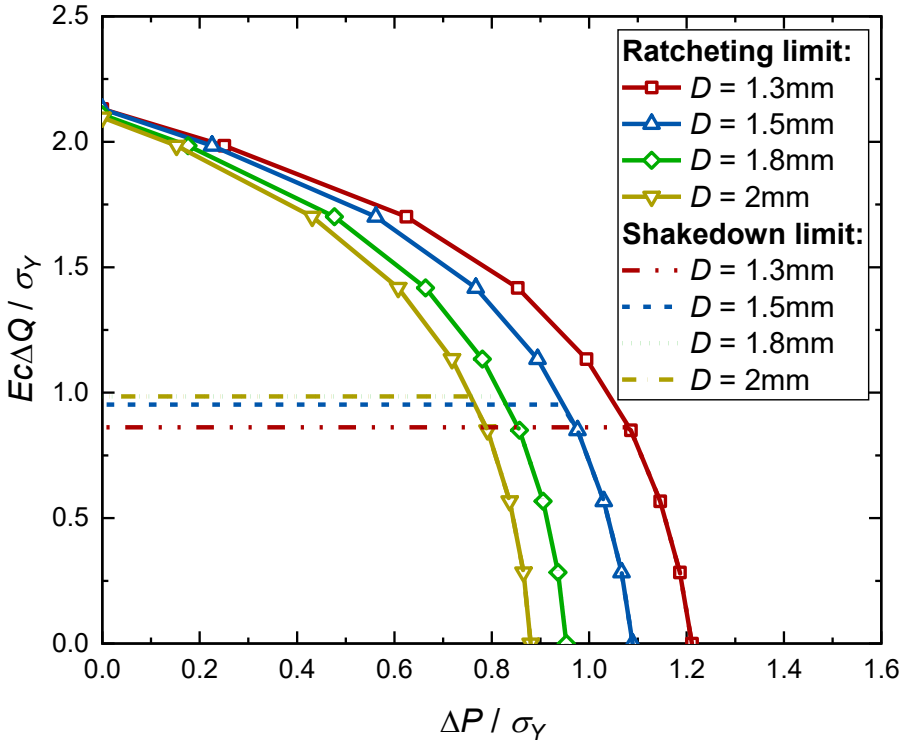

Fig.8 Shakedown and ratcheting boundaries for various channel diameters

5.2 Corner radius

A small corner radius is modeled instead of sharp corner of the semicircular channel. Various corner radii 0.5%, 1%, 2%, 3%, 4% and 5% of the channel diameter are included in analyses to demonstrate the influence of different corner radii. Shakedown and ratcheting analyses of 8×8 PCHE core with diameter 1.5mm of semielliptical channels subjected to differential pressures and temperatures are performed.

The shakedown and ratcheting boundaries for various core radii are presented in Fig.9. A magnified view of the bottom-right part of Fig.9 is presented in Fig.10 to show the differences among the curves. This indicates that corner radius influences the horizontal shakedown boundary (reverse plasticity limit associated with the local alternating plasticity) greatly, while it shows less effect on ratcheting boundary associated with the global ratcheting. When the corner radius varied from 0.5% to 5% of the channel diameter, the shakedown region gradually increases. This observation suggests that the corner radius of semicircular channel is an important factor in the shakedown investigation of PCHE core.

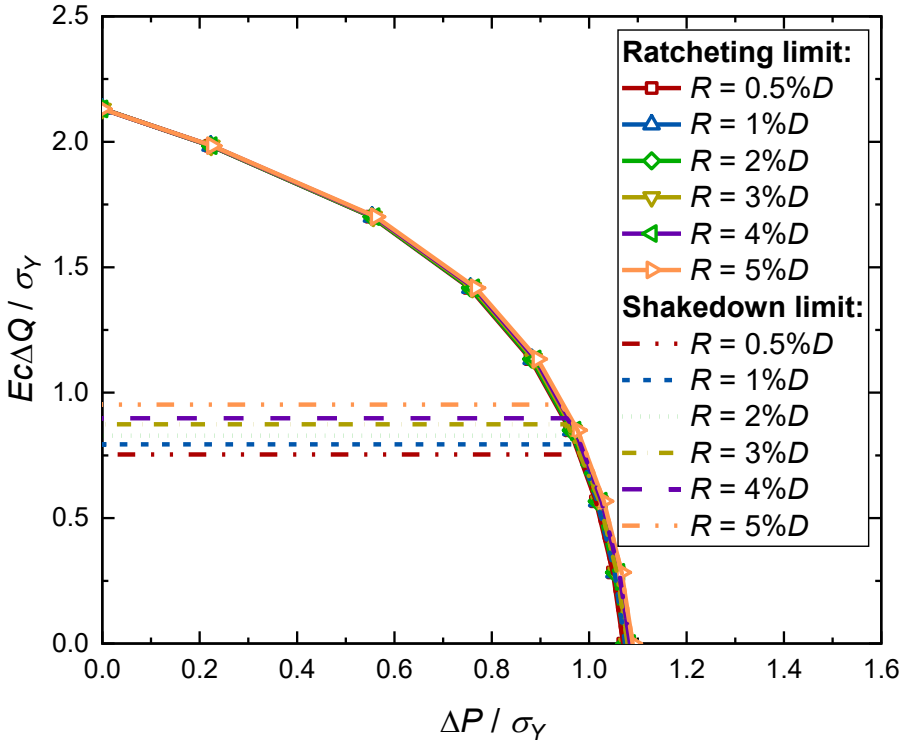

Fig.9 Shakedown and ratcheting boundaries for various core radii

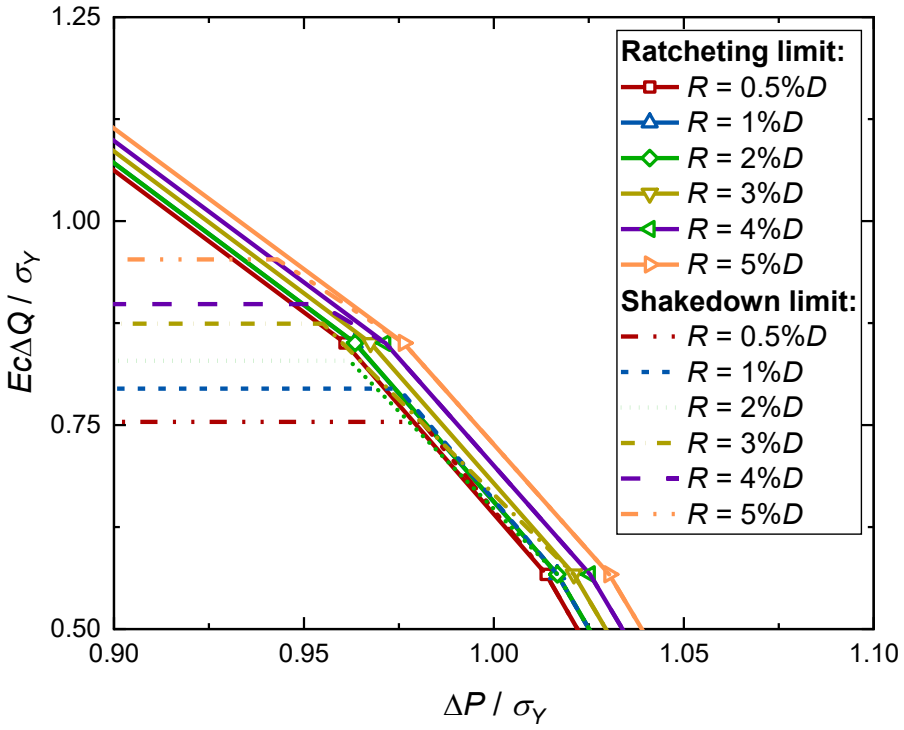

Fig.10 A magnified view of shakedown and ratcheting boundaries for various core radii

5.3 Core sizes

Various PCHE core sizes are also taken into consideration for analysis, as shown in Tab.2 . The diameter D is 1.5mm and corner radius is 5% D, other sizes are referred to Fig.4.

Tab.2 Different PCHE core sizes

Item	Number of rows m	Number of columns n
1	6	6
2	6	8
3	8	8
4	10	10
5	12	12
6	14	16
7	18	20

The results of shakedown and ratcheting boundaries for different core sizes are illustrated in Fig.11. The ratcheting boundary of PCHE model, which is influenced directly by the core size described as m×n, shifts markedly by increasing the core size, but the shakedown boundary changes relatively slightly with varying the core size. With the increase of PCHE core size, the bearing capacity is weakened, the shakedown region is reduced. Core size is crucial in the PCHE core design and influences shakedown and ratcheting behaviors significantly.

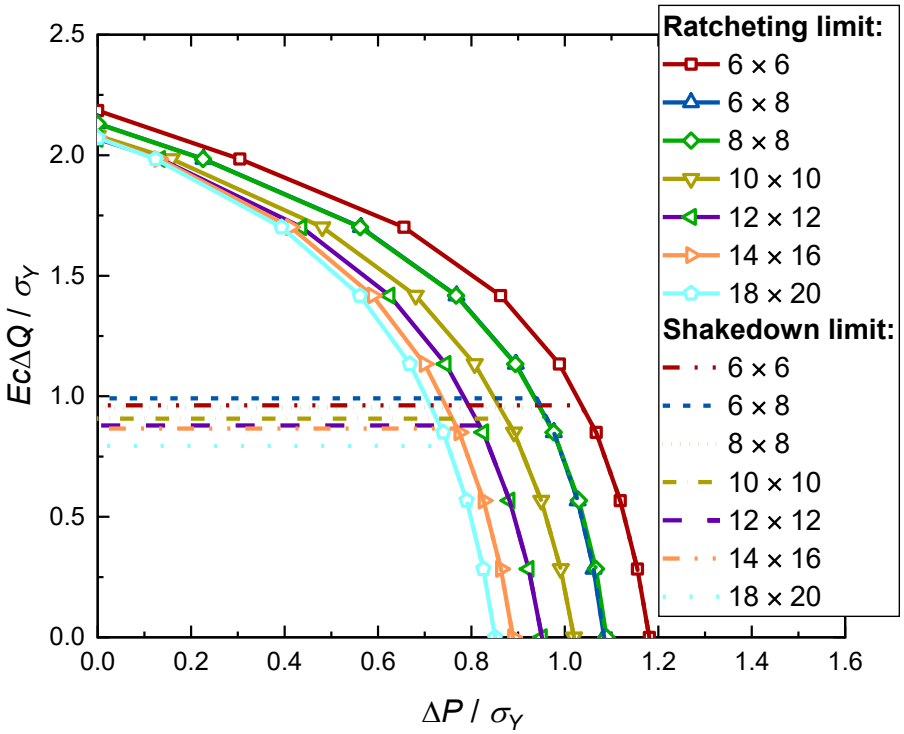

Fig.11 Shakedown and ratcheting boundaries for various core sizes

5.4 Channel shape

The semicircular channels may be distorted to semielliptical shapes after diffusion bonding process. Hence, a semielliptical shape of the channel is modeled as illustrated in Fig.12, with the sharp corner of 5%D. The mesh around the semielliptical shape of the channel is refined to simulate the stress change of structural discontinuities accurately. Shakedown and ratcheting analyses of 8×8 PCHE core with semielliptical channels subjected to differential pressures and temperatures are performed to investigate systematically the shakedown and ratcheting boundaries for PCHE core.

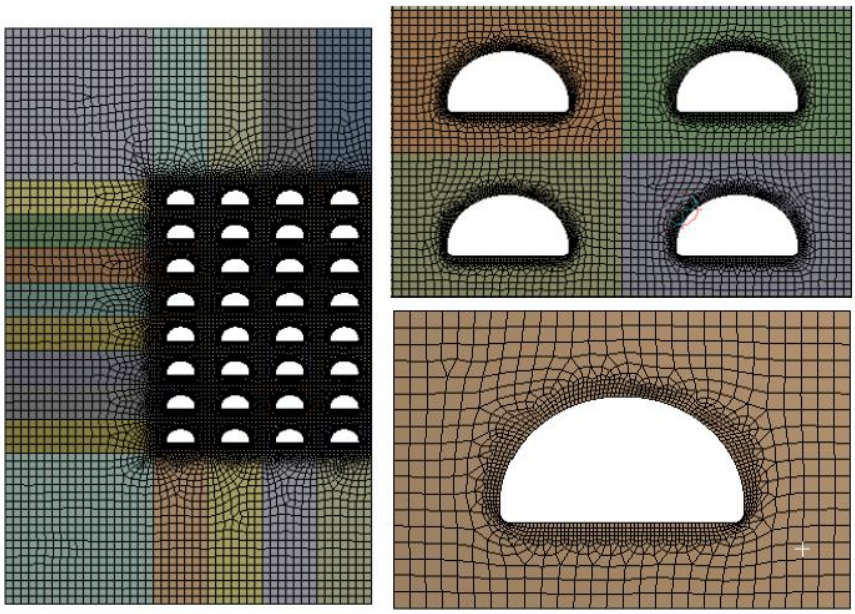

Fig.12 Semielliptical shape of a channel used in analysis

The shakedown and ratcheting limit boundaries of the semielliptical shape with the same core size obtained are compared to the result from semicircular channel analysis, as show in Fig.13. Results show that both the shakedown and ratcheting boundaries of the semielliptical shape are below those of semicircular shape. It can be indicated that the channel shape can make an effect on shakedown boundary, but little effect on ratcheting boundary. This is because that the semielliptical shape may induce additional stress concentration, leading to a lower reverse plasticity limit. These works can be very helpful for explaining the failure mechanism and establishing the safety assessment approach for the distorted semicircular channels after processed under repeated thermal loads.

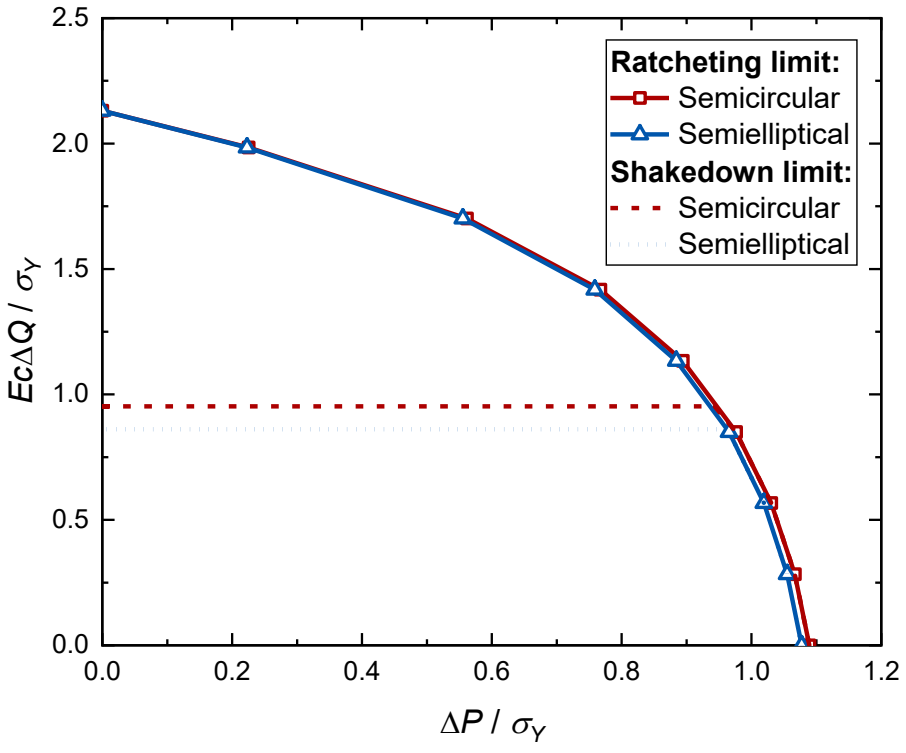

Fig. 13 The shakedown and ratcheting boundaries compared between semielliptical

shape and semicircular shape

5.5 Arrangements of channels

Different arrangements of channels are also studied to prove their effects on shakedown and ratcheting limit boundaries of PCHE core. There are two arrangements in common: triangle-type and square-type. As stated above, all PCHE models are modelled by square-type arrangement, whereas, a triangle-type arrangement of channels is modelled here, as illustrated in Fig. 14. All other parameters are the same as the benchmark model with core size 8×8.

The calculated shakedown and ratcheting limit boundaries for a triangle-type arrangement of channels are compared to the result for the square-type arrangement, as show in Fig.15. Results present that arrangements effect are non-negligible. Both the shakedown and ratcheting limit boundaries of the triangle-type arrangement are below those of square-type arrangement. The shakedown boundary is reduced from 0.95 to 0.71, and shows a relatively slight impact on the ratcheting limit boundary of PCHE core, as illustrated in Fig. 15. This is because that the triangle-type arrangement produces higher local stresses than the square-type arrangement.

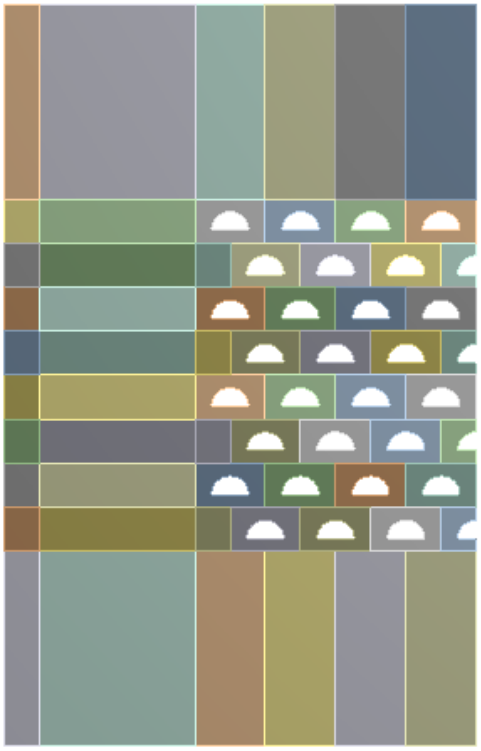

Fig. 14 Triangle-type arrangement of channel core

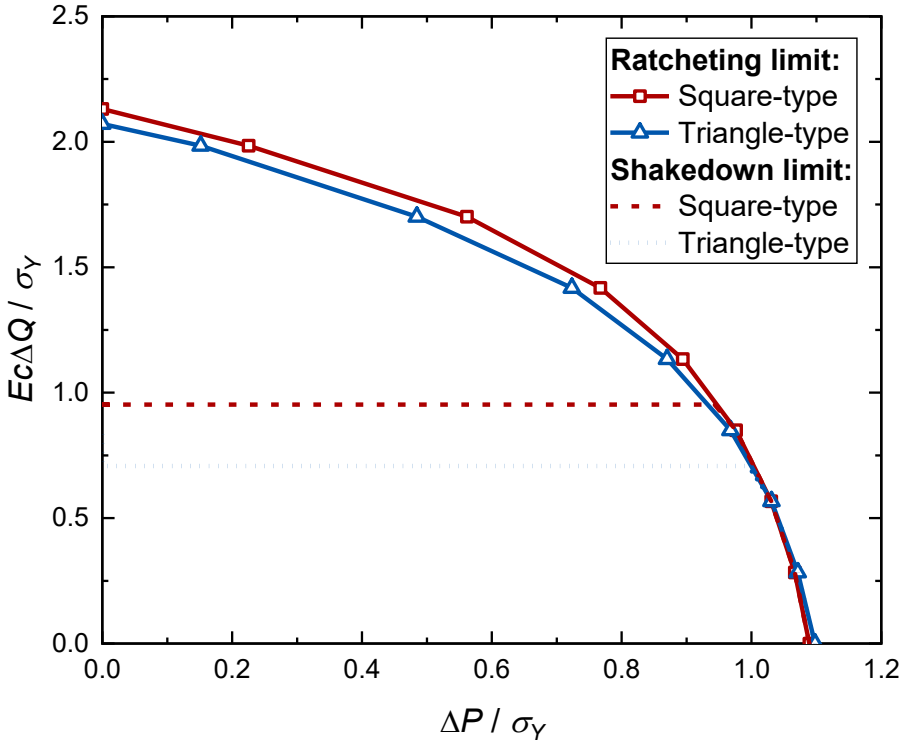

Fig. 15 The shakedown and ratcheting boundaries compared between different arrangements of channels

6 Conclusions

A new design and evaluation methodology for PCHEs for nuclear applications is proposed through the application of Linear Matching Method, and the LMM procedure can perfectly identify structural shakedown and ratcheting limit boundaries for elastoplastic solids under multi-dimensional periodic loading programs. Compared on the results of shakedown and ratcheting limit boundary of PCHE core with various structural parameters, a number of important conclusions can be obtained shown as below:

(a) Diameter of channel and core size are observed to have a significant influence on the ratcheting limit boundary, whereas a relatively little influence on the shakedown boundary. It is obvious that larger diameter of channel or core size can weaken the load bearing capacity of PCHEs. It is essential that diameter of channel and core size are optimized by parametric analysis during design stage.

(b) The variation of the corner radius from 0.5% to 5% of diameter of channel shows less effect on the ratcheting limit boundary associated with the global ratcheting, although it can significantly enlarges the shakedown region of PCHEs by inceasing the reverse plasticity limit.

(c) Shakedown and ratcheting boundaries of semielliptical channel cores are both lower than those of semicircular channel cores. The semicircular shape is a better choice. This indicates that the semielliptical channel should be avoided by strictly controlling manufacture process quality in diffusion bonding process.

(d) Different arrangement types of channels are observed to influence the shakedown responses significantly. By comparing the benchmark cases with the same core size and diameter of channel, the square-type arrangement is superior to triangle-type arrangement. Arrangement type influence on ratcheting limit boundary is not that significant, but it is found to have an

non-negligible effect on shakedown boundary.

It is worth noting that the results and conclusions from above parametric studies on PCHEs in the paper can provide a useful reference for structural design and optimization of PCHEs for high temperature nuclear applications.

Acknowledgments

The authors gratefully acknowledge the supports from the National Natural Science Foundation of China (51828501 and 52150710540), University of Shanghai for Science and Technology, East China University of Science and Technology and University of Strathclyde during the course of this work.

References

[1] Nestell J, Sham T L. ASME code considerations for the compact heat exchanger[J]. Oak Ridge National Laboratory, ORNL/TM-2015/401, 2015.

[2] Lee S M, Kim K Y. A parametric study of the thermal-hydraulic performance of a zigzag printed circuit heat exchanger[J]. Heat transfer engineering, 2014, 35(13): 1192-1200.

[3] Shen J, Chen H, Liu Y. A new four-dimensional ratcheting boundary: Derivation and numerical validation[J]. European Journal of Mechanics-A/Solids, 2018, 71: 101-112.

[4] Jentz I W, Anderson M H. A Flexible Tool for Modeling Thermal Loading in Printed Circuit Heat Exchangers[C]//Pressure Vessels and Piping Conference. American Society of Mechanical Engineers, 2019, 58943: V003T03A092.

[5] Katz A, Ranjan D. Advances Towards Elastic-Perfectly Plastic Simulation of the Core of Printed Circuit Heat Exchangers[C]//Pressure Vessels and Piping Conference. American Society of Mechanical Engineers, 2019, 58943: V003T03A093.

[6] Mahajan H P, Hassan T. Finite Element Analysis of Printed Circuit Heat Exchanger Core for Creep and Creep-Fatigue Responses[C]//Pressure Vessels and Piping Conference. American Society of Mechanical Engineers, 2019, 58967: V005T09A007.

[7] Mahajan H P, Devi U, Hassan T. Finite Element Analysis of Printed Circuit Heat Exchanger Core for High Temperature Creep and Burst Responses[C]//Pressure Vessels and Piping Conference. American Society of Mechanical Engineers, 2018, 51630: V03BT03A053.

[8] Hu H, Li J, Xie Y, et al. Experimental investigation on heat transfer characteristics of flow boiling in zigzag channels of printed circuit heat exchangers[J]. International Journal of Heat and Mass Transfer, 2021, 165: 120712.

[9] Hu H, Li J, Chen Y, et al. Measurement and correlation for two-phase frictional pressure drop characteristics of flow boiling in printed circuit heat exchangers[J]. International Journal of Refrigeration, 2021, 129: 69-77.

[10] YU GG Y, CHEN Y D. Study on the strength design of the plate of printed circuit heat exchanger[J]. Pressure Vessel Technology, 2018, 35(12): 42-46.

[11] Ishizuka T. Thermal-Hydraulic Characteristics of a Printed Circuit Heat Exchanger in a Supercritical CO_2 Loop[C]//The 11th International Topical Meeting on Nuclear Reactor Thermal-Hydraulics, 2005:218–232.

[12] Kim D E, Kim M H, Cha J E, et al. Numerical investigation on thermal–hydraulic performance of new printed circuit heat exchanger model[J]. Nuclear Engineering and Design, 2008, 238(12): 3269-3276.

[13] Natesan K, Moisseytsev A, Majumdar S. Preliminary issues associated with the next generation nuclear plant intermediate heat exchanger design[J]. Journal of nuclear materials, 2009, 392(2): 307-315.

[14] Mylavarapu S, Sun X, Figley J, et al. Investigation of high-temperature printed circuit heat exchangers for very high temperature reactors[J]. Journal of Engineering for Gas Turbines and Power, 2009, 131(6).

[15] Gai-Ge Y U , Chen Y D , Xue L I , et al. Research Progress in Heat Transfer and Fluid Flow of Printed Circuit Heat Exchanger[J]. Fluid Machinery, 2017.

[16] Xue L I , Yong-Dong C , Gai-Ge Y U , et al. Numerical Simulation on Thermal—hydraulic Performance of a Zigzag Printed Circuit Heat Exchanger[J]. Fluid Machinery, 2017.

[17] Chen H, Ponter A R S. A direct method on the evaluation of ratchet limit[J]. Journal of Pressure Vessel Technology, 2010, 132(4).

[18] Chen H F, Ponter A R S, Ainsworth R A. The linear matching method applied to the high temperature life integrity of structures. Part 2. Assessments beyond shakedown involving changing residual stress fields[J]. International Journal of Pressure Vessels and Piping, 2006, 83(2): 136-147.

[19] Gong J G , Niu T Y , Chen H , et al. Shakedown analysis of pressure pipeline with an oblique nozzle at elevated temperatures using the linear matching method[J]. International Journal of Pressure Vessels and Piping, 2018, 159:55-66.

[20] Zhu X , Chen H , Xuan F , et al. Cyclic plasticity behaviors of steam turbine rotor subjected to cyclic thermal and mechanical loads[J]. European Journal of Mechanics - A/Solids, 2017, 66:243-255.

[21] Bradford R , Tipping D J . The Ratchet-Shakedown Diagram for a Thin Pressurised Pipe Subject to Additional Axial Load and Cyclic Secondary Global Bending[J]. International Journal of Pressure Vessels and Piping, 2015, 134:92-100.

[22] Santanna R , Zouain N . A direct method for ratchet boundary determination[J]. European Journal of Mechanics - A/Solids, 2019, 75:156-168.

[23] ASME Boiler & Pressure Vessel Code, Section VIII Rules for Construction of Pressure Vessels 2019.

[24] ASME Boiler & Pressure Vessel Code, Section III, Rules for Construction of Nuclear Facility Components 2019.

[25] Ponter A R S, Engelhardt M. Shakedown limits for a general yield condition: implementation and application for a von Mises yield condition[J]. European Journal of Mechanics-A/Solids, 2000, 19(3): 423-45.

[26] Ma Z, Chen H, Liu Y, et al. A direct approach to the evaluation of structural shakedown limit considering limited kinematic hardening and non-isothermal effect[J]. European Journal of Mechanics-A/Solids, 2020, 79:103877.

[27] Barbera D, Chen H, Liu Y, et al. Recent developments of the linear matching method framework for structural integrity assessment[J]. Journal of Pressure Vessel Technology, 2017, 139(5).

[28] Cho N K, Chen H. Shakedown, ratchet, and limit analyses of 90 back-to-back pipe bends under cyclic in-plane opening bending and steady internal pressure[J]. European Journal of Mechanics-A/Solids, 2018, 67:231-42.